J. Amr. Uni. 04 (2024) p.167

Dynamics of SIR Model on Random Networks

M. Ali Saif[1,*], M. A. Shukri[2,†] and F. H. Al-makhedhi[2,‡]
[1] Department of Physics,University of Amran, Amran,Yemen.
[2] Department of Physics, University of Sana'a, Sana'a, Yemen.

Abstract

we focus on studying the dynamics of infectious disease spreading SIR model on random networks. We investigate how various parameters of the network influence the behavior of spreading and analyze the occurrence of phase transitions within this network framework. Our analysis reveals the critical role of network connectivity in shaping the dynamics of disease transmission and highlights the presence of mean-field phase transitions. Additionally, we employ both analytical techniques and simulation methods to extract critical thresholds for the model and compare them for validation. By delving into the intricate dynamics of disease spreading on random networks, this work offers valuable insights into the mechanisms driving epidemic propagation and provides a theoretical foundation for studying disease control strategies and public health interventions.

1 Introduction

Because many real-world phenomena incorporate spreading dynamics on complex networks, the topic has received much attention over the last decade [1, 2]. Notable examples include the spread of transmitted diseases through contact networks,the spread of malware on wireless networks, and the spread of computer viruses through email networks. In each case the spreading dynamics are strongly affected by *network topology*, and this complicates the task of understanding their behavior. Existing studies of spreading dynamics have focused on both theoretical aspects (e.g., nonequilibrium critical phenomena) and practical issues (e.g., proposing efficient immunization strategies). Researchers have focused on developing ways of accurately identifying epidemic thresholds because of their important ramifications in many real-world scenarios [3, 4]. Theoretically speaking, an epidemic threshold characterizes the critical condition above which a global epidemic occurs. Being able to predict an epidemic threshold allows us to determine the critical exponents and Griffiths effects, which are important in research on nonequilibrium phenomena. Practically speaking, quantifying an epidemic threshold allows us to determine the effectiveness of a given immunization strategy. A proposed immunization strategy is effective if it increases the epidemic threshold. In addition, knowing the epidemic threshold enables us to more accurately determine the optimum source node [5].

A fundamental question in the study of epidemics is whether a disease will spread throughout a population or die out. This depends on factors such as infection and recovery rates, as well

*E-mail:masali73@gmail.com
†E-mail:mshukri2006@gmail.com
‡E-mail:fatymeheod@gmail.com

as the structure of connections between individuals. For the SIR model on many kinds of networks, the epidemic threshold and the critical infection rate above which the disease infects a nonzero fraction of the population were previously derived [6, 7]. In this chapter we study the model of epidemic spreading SIR model on random networks.

2 Model and Methods

The SIR model of epidemic spreading on the networks can be described as follows [8]: Consider a population of N individuals living at the sites of a one dimensional lattice. The individual can be in one state of three states, susceptible (S), infected (I) and refractory (R). The interaction between the nodes on the lattice occurs as follows: the nodes in the state I on the network can infect any one of their neighbours which are in state S with probability λ at each time step. The nodes in state I pass to the state R after an infection time τ_I. During the R phase, the nodes are immune and do not infect. The dynamics of the model are summarized as

$$S + I \xrightarrow{\lambda} I + I, I \xrightarrow{\tau_I} R, \tag{1}$$

In this work we follow Grassberger's second model in Ref. [8] and we set $\tau_I = 1$. This model will evolve ultimately to the state where there are no infected individuals in the lattice, which will happen for any initial state of I individuals and any values of infection probability λ. That means the final state of this model is a mixture of S and R individuals. Therefore, this state which is free of infected individuals is the absorbing state of this model. To evaluate to what extent the infection has spread within the nodes of the network, we use the density of refractory nodes $\langle\rho\rangle$ as a measure for that. This quantity is called also the order parameter of the system, which can be defined as follows

$$\langle\rho\rangle = \frac{N_R}{N} \tag{2}$$

where N is the total number of lattice sites, N_R is the total number of lattice sites in state R, and $\langle\rho\rangle$ stands for the average over different network realizations.

We construct the random network using the Erdös-Rényi (ER) [9] method. A random network is defined as follows [10]: initially, we have N isolated nodes, with each pair of nodes connected with a probability p. This leads to a Poisson degree distribution $P(k) = e^{-\langle k\rangle}\frac{\langle k\rangle^k}{k!}$, where the average degree (connectivity) is determined by

$$\langle k\rangle = pN \tag{3}$$

This quantity plays a pivotal role in these types of networks. Depending on the value of $\langle k\rangle$, we can discern between three cases.

1. In the case when $\langle k\rangle = pN < 1$ the graph is composed of an isolated tree.
2. The case when $\langle k\rangle > 1$ a giant cluster appears.
3. The case when $\langle k\rangle \geq \ln(N)$ the graph is totally connected.

Fig. 1 depicts this behavior of a random network, where we visualize the random network for three different values of connectivity $\langle k\rangle = 0.9, 2.0$ and 6.0 for a lattice of size $N = 100$ sites.

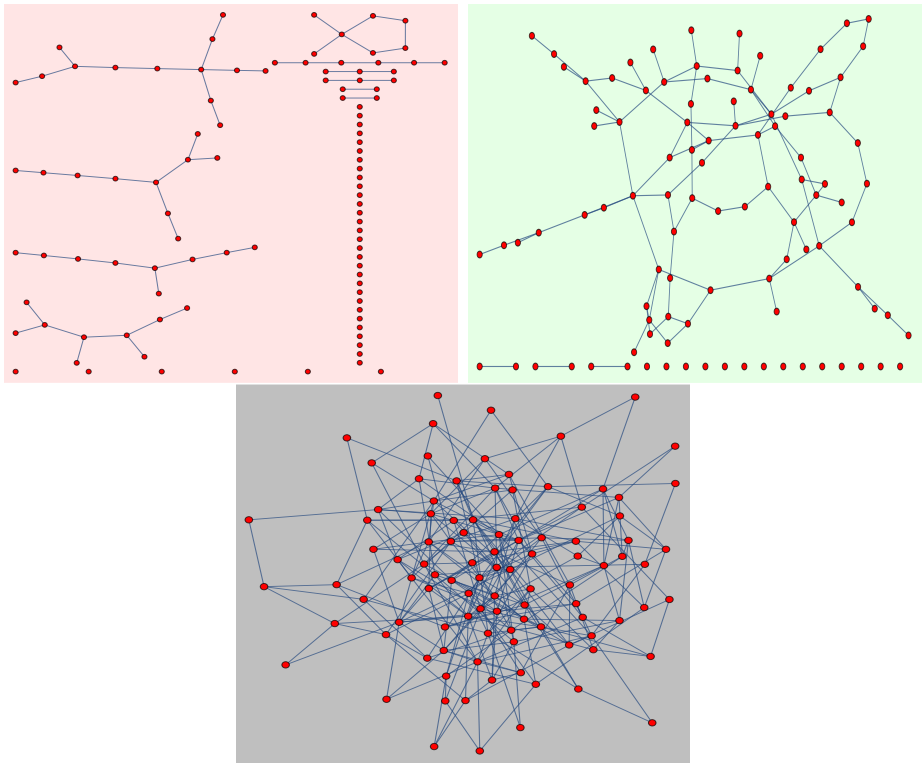

Figure 1: Random network for three values of connectivity $\langle k \rangle = 0.9, 2.0$ and 6.0 for a lattice of size $N = 100$ sites.

3 Spreading on random networks

In this section, we examine how the infection spreads among nodes in the random network. To measure this, we utilize the density of immune nodes, denoted as $\langle \rho \rangle$ (Eq. (2)). We conduct simulations of our model across various values of connectivity, denoted as $\langle k \rangle$, and infection probability, denoted as λ. In our simulations of the SIR model, we employ a lattice comprising $N = 10^4$ sites and allow the system to evolve until all infected nodes are cleared. We compute the average density of immune nodes over 1000 different configurations. Fig. 2 illustrates the density of immune nodes, $\langle \rho \rangle$, as a function of the infection probability, λ, for various values of connectivity, $\langle k \rangle$, categorized as follows: $\langle k \rangle < 1$, $1 < \langle k \rangle < \ln(N)$, and $\langle k \rangle \geq \ln(N)$. The figure depicts how the density of immune sites changes as λ varies from 0 to 1.

The observations from the figure are as follows:

1. When $\langle k \rangle < 1$, the spreading remains localized, with only a few sites becoming infected.
2. For $1 < \langle k \rangle < \ln(N)$, the spreading enlarges, although a significant number of nodes remain uninfected.
3. When $\langle k \rangle \geq \ln(N)$, the spreading becomes global, leading to the infection of all nodes.

This behavior mirrors the underlying structure of the network, contingent upon the value of connectivity, $\langle k \rangle$.

We further validate the previous findings by examining the density of immune nodes, denoted as $\langle \rho \rangle$, as a function of connectivity, $\langle k \rangle$, as shown in Fig. 3. In these simulations of the model, we fix the value of λ to be $\lambda = 1$. The figure clearly illustrates the three distinct regions of spreading.

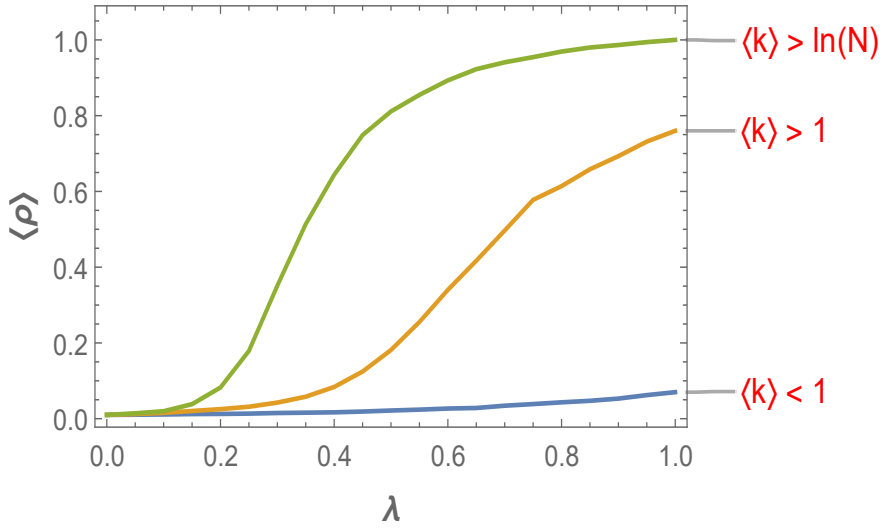

Figure 2: Density of immune nodes $\langle\rho\rangle$ as a function of infection probability λ at various values of connectivity $\langle k\rangle$.

4 Phase transition and critical behavior

In this section, our focus is on studying the nonequilibrium phase transition of the SIR model on random networks. We specifically examine the region where the network becomes connected, i. e., $\langle k\rangle \geq \ln(N)$. Our objective is to derive the analytical expression for the critical threshold of this model on random networks.

4.1 Epidemic Critical Threshold

To derive the epidemic threshold [7], we require some definitions from percolation theory. In a percolation process on a network, links are systematically removed until only a fraction q of the N network nodes remain. This process continues until a critical value, known as the percolation threshold q_c, is attained. When $q > q_c$, a spanning cluster comprising a significant fraction of the N nodes emerges, whereas for $q < q_c$, the network fragments into smaller clusters [9, 11].

Disease spreading can be conceptualized as a growing percolation process [12], wherein, starting from a given seed, links are progressively added to the expanding network with a certain probability q. The critical infection rate at which the disease spreads throughout the network corresponds to the percolation threshold at which a spanning cluster emerges. To establish this analogy, we need to define the epidemic equivalent of q, which represents the probability of a node infecting its neighbour. This probability differs from λ, as an infected node i can transmit the infection to its neighbour j only while it remains infected for a duration of τ_I time steps. Hence, the desired probability is given by [13, 14, 15]:

$$q = 1 - (1 - \lambda)^{\tau_I} \tag{4}$$

The critical infection rate λ_c for a given τ_I can then be obtained by substituting the value of q_c in Eq. (4).

To obtain q_c, we define $\langle n_i\rangle$, the average number of susceptible nodes infected by an already infected node i. If $\langle n_i\rangle > 1$, the disease will keep on spreading until a nonzero fraction of the network is covered [16]. To show this behavior for the SIR model on random networks, in Fig.

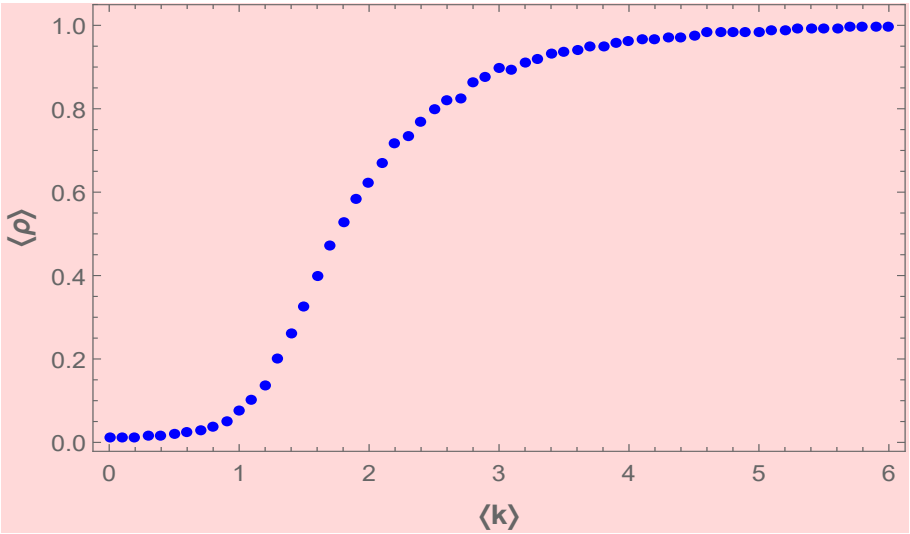

Figure 3: Density of immune nodes $\langle\rho\rangle$ as a function of connectivity $\langle k\rangle$ when $\lambda = 1$.

4, we plot the density of immune nodes $\langle\rho\rangle$ as a function of infection probability λ. Simulation in this figure is done using a lattice of size $N = 10^3$ and $p = 0.01$ averaged over 1000 realization. It is clear from the figure the value of $\langle\rho\rangle$ depends on the value of λ. For small values of λ the number of infected nodes is approximately zero, however as the value of λ becomes greater than $\lambda > 0.1$ the density of immune nodes $\langle\rho\rangle$ increases. Using Fig. 4, we can estimate the critical point to be $\lambda_c = 0.1$ in this case (see Inset of Fig. 4). We can confirm this value of the critical point analytically. Whereas the average number of numbers of any node on the network will be $\langle k\rangle = pN = 10$. Therefore, the average number of susceptible nodes $\langle n_i\rangle$ infected by an already infected node i will be $\langle n_i\rangle = \lambda\langle k\rangle$. Using the condition $\langle n_i\rangle > 1$. Then $\lambda_c = 0.1$ which coincides exactly with the numerical value.

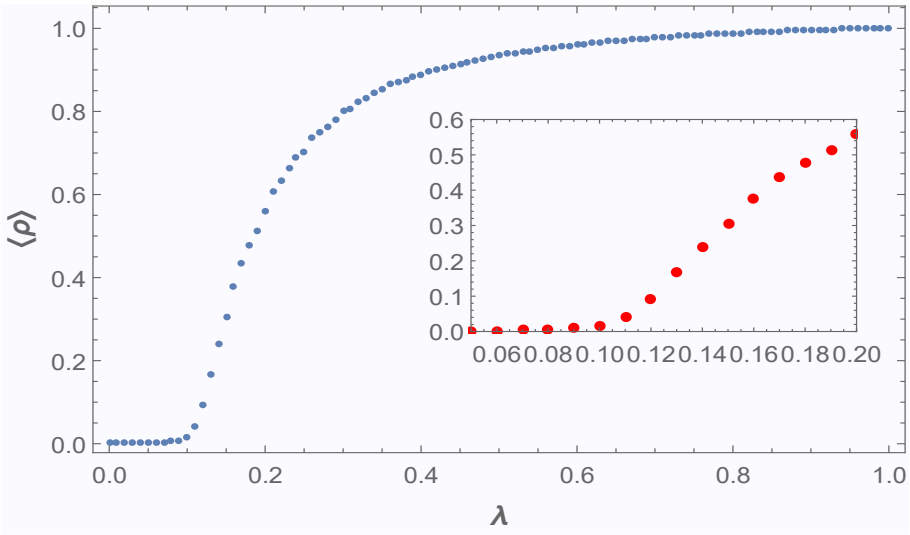

Figure 4: Density of immune nodes $\langle\rho\rangle$ as a function of λ, for $N = 10^3$ and $p = 0.01$.

In general we are going here to find the analytical expression for the critical threshold of this model on random networks [7]. The probability of a node reached by following a link to have degree k (comprising one incoming link and $k-1$ outgoing links) is $kP(k)/\langle k\rangle$, where

$P(k)$ represents the degree distribution of the network nodes. Therefore, under the assumption of a treelike structure with negligible loops [18], the average number of neighbours infected by node i can be expressed as [16]:

$$\langle n_i \rangle = q \sum_k \frac{kP(k)}{\langle k \rangle}(k-1) = q(\kappa - 1) \tag{5}$$

where $\kappa - 1 \equiv [\langle k^2 \rangle / \langle k \rangle] - 1$ is the branching factor. At the epidemic threshold, $q_c(\kappa - 1) = 1$. So the critical threshold in this is

$$q_c = \frac{1}{\kappa - 1} \tag{6}$$

Substituting the value of q_c from Eq. (6) into Eq. (4), we obtain the following equation for the critical threshold λ_c:

$$\lambda_c = 1 - (\frac{\kappa - 2}{\kappa - 1})^{1/\tau_I} \tag{7}$$

For the case when $\tau_I = 1$, the previous equation simplifies to:

$$\lambda_c = \frac{1}{\kappa - 1} \tag{8}$$

To assess the accuracy of the previous equation, we will utilize Eq. (8) to determine the critical points of this model on random networks and compare them with the critical points obtained through Monte Carlo simulations. In the simulations, we will extract the critical points like what was done in Fig. 4. It's worth noting that while the method used here provides critical points, the most accurate method for determining them is the one employed in Ref. [17]. However, the method used here yields critical points albeit with slightly less accuracy.

Table 1: Critical points for the SIR model on a random network.

$\langle k \rangle$	λ_c simulation results	λ_c from Eq. (8).
7.0	0.156(4)	0.1667
10.0	0.105(3)	0.1111
13.0	0.085(3)	0.0833
17.0	0.063(2)	0.0625
21.0	0.051(2)	0.0500
26.0	0.041(2)	0.0400
33.0	0.032(2)	0.0312
41.0	0.024(2)	0.0250
51.0	0.021(1)	0.0200
66.0	0.016(2)	0.0153
101.0	0.010(1)	0.0100

In Table 1, we summarize the estimated values of the critical points obtained from our Monte Carlo simulations and Eq. (8) for various values of connectivity $\langle k \rangle$. Fig. 5 illustrates the comparison between the critical points determined through Monte Carlo simulations and those obtained using Eq. (8). The figure demonstrates an excellent correspondence between the simulation results and the analytical relation given by Eq. (8).

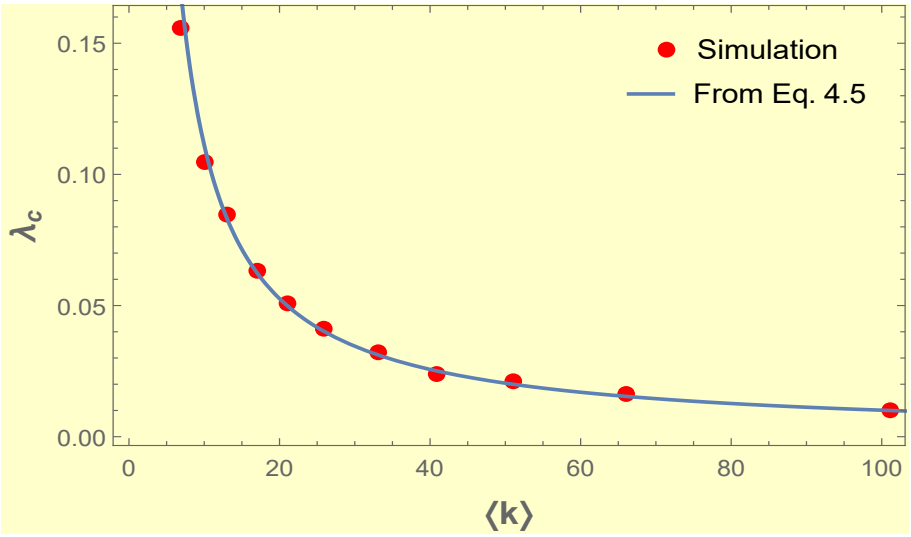

Figure 5: Simulation results of the critical points λ_c (represented by circles) for $N = 10^3$, alongside the theoretical critical threshold obtained from Eq. (8), are plotted as a function of connectivity $\langle k \rangle$.

4.2 Phase transition and critical exponents

The behavior observed in the previous section indicates that the SIR model on random networks undergoes a phase transition from an absorbing phase to an active phase at the critical point λ_c. To determine the nature of this phase transition, we numerically calculate the values of some critical exponents of this system. It is known that absorbing phase transitions are characterized by four independent critical exponents $\beta, \acute{\beta}, \nu_\perp$, and $\nu_{||}$. However, the DyP class exhibits a symmetry known as rapidity reversal symmetry, implying that $\beta = \acute{\beta}$ [19]. Thus, DyP is characterized by only three critical exponents instead of four, with all other exponents expressible in terms of these. The dynamic exponent z is given by $z = \nu_{||}/\nu_\perp$. Additionally, the exponents δ, α, and θ are determined by $\delta = \acute{\beta}/\nu_{||}$, $\alpha = \beta/\nu_{||}$, and $\theta = d/z - 2\delta$, where d denotes the system's dimension [19].

It is established that for continuous phase transitions, the stationary value of the order parameter $\langle \rho \rangle$ diminishes asymptotically as the control parameter λ approaches a critical value λ_c, following a power law, characterized by:

$$\langle \rho \rangle \approx (\lambda - \lambda_c)^\beta \tag{9}$$

The exponent β can be determined by plotting the value of $\langle \rho \rangle$ as a function of $(\lambda - \lambda_c)$ on a logarithmic scale (refer to Fig. 6). The power law behavior becomes evident, and the best-fit value of the critical exponent is found to be $\beta = 1.0 \pm 0.0001$, which remarkably matches the theoretical value of $\beta = 1.0$ reported in [20] for the mean field of the DyP universality class. This compatibility with the DyP mean field leads us to conjecture that the SIR model on random networks belongs to the mean field of the dynamical percolation universality class.

4.3 Time-dependent simulation

To ascertain the universality class of this model, we delve into further critical exponents in this section. Discerning the nature of phase transitions is somewhat an 'asymptotic' endeavour,

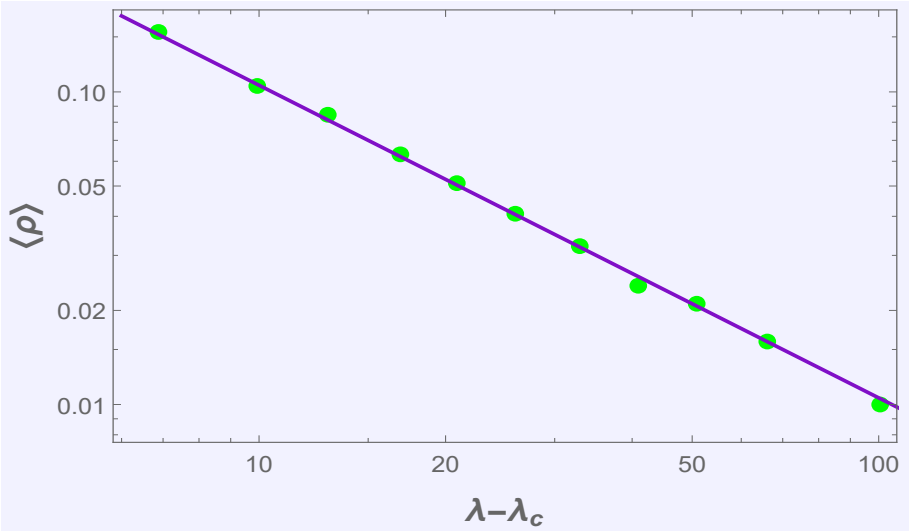

Figure 6: Stationary density of immune sites $\langle\rho\rangle$ as a function of the distance to the critical point on a double logarithmic scale, when $\langle k\rangle = 10$. The linear result accurately fits to the numerically obtained data with the exponent $\beta = 1.0 \pm 0.001$.

where we make conjectures about the asymptotic behaviour of thermodynamic systems by systematically simulating systems of finite size for finite durations. Fortunately, some insights into the transition's nature can be gleaned from time-dependent dynamics, as elucidated in Ref. [17]. In this approach, we initiate simulations from a configuration close to the absorbing state, which, in our case, entails commencing simulations from a single active site at the centre of the lattice. We monitor the time evolution of the system, which begins very near the absorbing state configuration. We numerically track the survival probability $P(t)$ (the likelihood that the system doesn't reach the absorbing state until time t) and the average number of active sites $N(t)$. At the critical point, these quantities are expected to exhibit asymptotic power laws (refer to Ref. [17] and the references therein). To ascertain the critical exponents more precisely, we employ the local slope method, introducing the effective exponent as defined in Ref. [17]).

In the simulation of the SIR model here, we utilize a lattice of size $N = 10^5$ and average over 2000 initial conditions, with $m = 4$ fixed. In Figs. 7, we depict the value of the effective exponent θ as a function of $1/t$, with the top plot showcasing results when $\langle k\rangle = 13$, and the bottom plot presenting results for $\langle k\rangle = 23$. It is evident that for $\lambda \neq \lambda_c$, the values tend towards zero or diverge to infinity, while they converge to a constant value precisely at $\lambda = \lambda_c$. The estimated value of $\theta = 0.0 \pm 0.001$ demonstrates excellent agreement with the exponents for the DyP mean field within the error bars.

Fig. 8 depict the value of the effective exponent δ as a function of $1/t$, with the top plot representing results when $\langle k\rangle = 13$, and the bottom plot showcasing results for $\langle k\rangle = 23$. Similarly to the previous case, it is evident that for $\lambda \neq \lambda_c$, the values tend towards zero or diverge to infinity, while they converge to a constant value precisely at $\lambda = \lambda_c$. The estimated value of $\delta = 1.001 \pm 0.002$ also demonstrates excellent agreement with the exponents for the DyP mean field within the error bars.

In Table 2, we summarize the results of critical points obtained in this study and compare them with the exact values of critical exponents for the DyP mean field. The three critical exponents we have calculated, namely β, θ, and δ, affirm that the nonequilibrium phase tran-

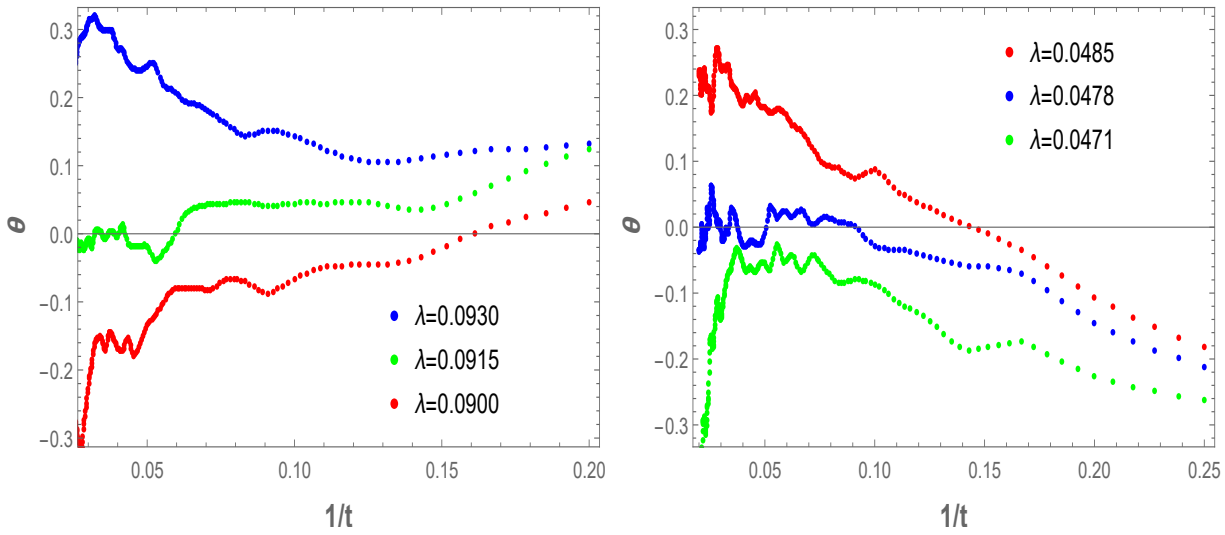

Figure 7: Time dependent behavior of the effective exponent θ as a function of $1/t$, left: when $\langle k \rangle = 13$ and right: when $\langle k \rangle = 23$.

sition of the SIR model on random networks belongs to the mean field of the DyP universality class.

Table 2: Critical exponents for the SIR model on a random network.

	β	θ	δ
Exact value [20]	1.0	0.0	1.0
This work	1.00±0.001	0.0±0.001	1.00±0.002

References

[1] A. Barrat, M. Barthélemy and A. Vespignani, Dynamical processes on complex networks (Cambridge University Press, Cambridge, UK 2008), 1st ed.

[2] C. Castellano, S. Fortunato and S. Fortunato, Statistical physics of social dynamics. Rev. Mod. Phys. **81**, 0034 (2009).

[3] G. Ódor, Rev. Mod. Phys. **76**, 663 (2004).

[4] M. Ali Saif, Scientific Reports **13**, 21555 (2023).

[5] W. Wang, Q.-H. Liu1, L.-F. Zhong, M. Tang, H. Gao and H. E. Stanley, Scientific Reports **6**, 24676 (2016).

[6] R. Pastor-Satorras and A. Vespignani, Phys. Rev. Lett. **86**, 3200 (2001).

[7] R. Parshani, S. Carmi, and S. Havlin, Phys Rev. Lett. **104**, 258701 (2010).

[8] P. Grassberger, Mathematical Biosciences **63**, 157 (1983).

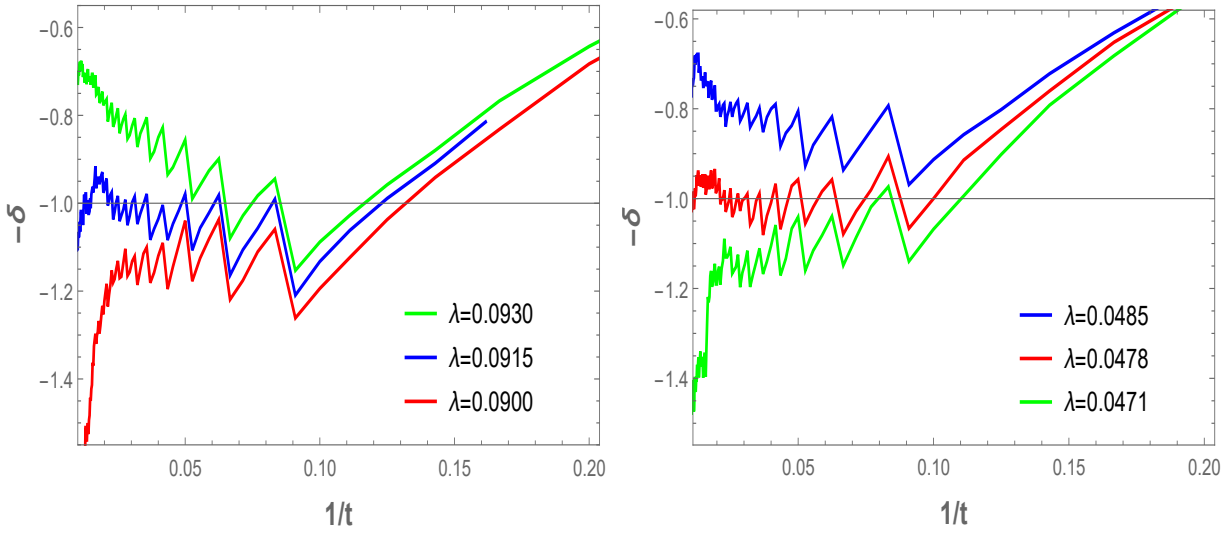

Figure 8: Time dependent behavior of the effective exponent δ as a function of $1/t$, left: when $\langle k\rangle = 13$ and right: when $\langle k\rangle = 23$.

[9] P. Erdös and A. Rényi, Publ. Math. Debrecen **6**, 290 (1959).

[10] M. Ali Saif, J. Amr. Uni. **01**, 176-184 (2021).

[11] D. Stauffer and A. Aharony, Introduction to Percolation Theory (Taylor & Francis, London, 2004), 2nd ed.

[12] Z. Alexandrowicz, Phys. Lett. A **80**, 284 (1980).

[13] M. E. J. Newman, Phys. Rev. E **66**, 016128 (2002).

[14] J. L. Cardy and P. Grassberger, J. Phys. A: Math. Gen. **18**, L267 (1985).

[15] G. Yan, Zhong-Qian Fu, Jie Ren and Wen-Xu Wang, Phys. Rev. E **75**, 016108 (2007).

[16] N. Madar, T. Kalisky, R. Cohen, D. Ben-Avraham, and S. Havlin, Eur. Phys. J. B **38**, 269 (2004).

[17] M. A. Saif, M. A. Shukri, F. H. Al-makhedhi, Physica A **633**, 129430 (2024).

[18] R. Cohen, K. Erez, D. ben Avraham, and S. Havlin, Phys. Rev. Lett. **85**, 4626 (2000).

[19] H. Hinrichsen, Adv. Phys. **49**, 815 (2010).

[20] M. A. Muñoz, R. Dickman, A. Vespignani and S. Zapperi, Phys. Rev. E (brief reports) 59, 6175(1999).